Naval Research Laboratory
Washington, DC 20375-5320

NRL/7220/MR—2023/3

Remote Detection of Overwintering Fires

CHRISTOPHER SELMAN

Passive Microwave Branch
Remote Sensing Division

November 13, 2023

REPORT DOCUMENTATION PAGE

Form Approved
OMB No. 0704-0188

1. REPORT DATE *(DD-MM-YYYY)*	**2. REPORT TYPE**	**3. DATES COVERED** *(From - To)*
13-11-2023	NRL Memorandum Report	15-07-2022 – 15-07-2023

4. TITLE AND SUBTITLE

Remote Detection of Overwintering Fires

5a. CONTRACT NUMBER

5b. GRANT NUMBER

5c. PROGRAM ELEMENT NUMBER
NISE

6. AUTHOR(S)

Christopher Selman

5d. PROJECT NUMBER

5e. TASK NUMBER

5f. WORK UNIT NUMBER
2201

7. PERFORMING ORGANIZATION NAME(S) AND ADDRESS(ES)

Naval Research Laboratory
4555 Overlook Avenue, SW
Washington, DC 20375-5320

8. PERFORMING ORGANIZATION REPORT NUMBER

NRL/7220/MR--2023/3

9. SPONSORING / MONITORING AGENCY NAME(S) AND ADDRESS(ES)

Naval Research Laboratory
4555 Overlook Avenue, SW
Washington, DC 20375-5320

10. SPONSOR / MONITOR'S ACRONYM(S)

NRL-NISE

11. SPONSOR / MONITOR'S REPORT NUMBER(S)

12. DISTRIBUTION / AVAILABILITY STATEMENT

DISTRIBUTION STATEMENT A: Approved for public release; distribution is unlimited.

13. SUPPLEMENTARY NOTES

Karles Fellowship

14. ABSTRACT

This report presents research conducted by Dr. Christopher Manuel Selman over July 18 th , 2022, to July 18 th , 2023, for his Karle's Fellowship in Detecting Overwintering Arctic Fires. Overwintering fires are fires that span two years; in the first year, there is an incipient fire. This fire burns deep into the peat of boreal forests and smolders over the winter, into the next thaw. After the ground has thawed, the fire re-emerges. Currently, remote detection or even simple identification of overwinters is difficult. For detection, persistent cloud cover, snow cover and frozen soil present insurmountable odds for any one wavelength to overcome. A multispectral approach, utilizing low earth orbiting visible, infrared and microwave instruments may mitigate these weaknesses. However, before any analysis can begin, case studies must first be identified. In this study, I discuss the development of a parsing tool for Alaskan Wildland Fire Information data using a series of Python routines. One candidate fire of suitable size identified from this utility and another fire from the literature are chosen for analysis. Data from the Visible Infrared Imaging Radiometer Suite (VIIRS) and Soil Moisture Active Passive (SMAP) instruments are then ingested into newly developed capabilities of the Navy's Geolocated Information Processing Suite (GeoIPS.) These capabilities include a normalized burn ratio and VIIRS Day Land Cloud Fire RGB, as well as microwavebrightness temperature plots from the SMAP passive microwave radiometer and synthetic aperture radar.

15. SUBJECT TERMS

16. SECURITY CLASSIFICATION OF:			**17. LIMITATION OF ABSTRACT**	**18. NUMBER OF PAGES**	**19a. NAME OF RESPONSIBLE PERSON**
					Christopher Selman
a. REPORT	**b. ABSTRACT**	**c. THIS PAGE**	U	26	**19b. TELEPHONE NUMBER** *(include area code)*
U	U	U			(202) 767-1937

This page intentionally left blank.

CONTENTS

FIGURES

TABLES

EXECUTIVE SUMMARY

This report presents research conducted by Dr. Christopher Manuel Selman over July 18th, 2022, to July 18th, 2023, for his Karle's Fellowship in Detecting Overwintering Arctic Fires. Overwintering fires are fires that span two years; in the first year, there is an incipient fire. This fire burns deep into the peat of boreal forests and smolders over the winter, into the next thaw. After the ground has thawed, the fire re-emerges. Currently, remote detection or even simple identification of overwinters is difficult. For detection, persistent cloud cover, snow cover and frozen soil present insurmountable odds for any one wavelength to overcome. A multispectral approach, utilizing low earth orbiting visible, infrared and microwave instruments may mitigate these weaknesses. However, before any analysis can begin, case studies must first be identified. In this study, I discuss the development of a parsing tool for Alaskan Wildland Fire Information data using a series of Python routines. One candidate fire of suitable size identified from this utility and another fire from the literature are chosen for analysis. Data from the Visible Infrared Imaging Radiometer Suite (VIIRS) and Soil Moisture Active Passive (SMAP) instruments are then ingested into newly developed capabilities of the Navy's Geolocated Information Processing Suite (GeoIPS.) These capabilities include a normalized burn ratio and VIIRS Day Land Cloud Fire RGB, as well as microwave brightness temperature plots from the SMAP passive microwave radiometer and synthetic aperture radar. While I was unable to detect overwinters with these tools, several important observations were made regarding fire tracking and emergence. From these results it should be possible to automate new and resuming fire detection. Further, I explain how the tools developed here can slot into the operational flow of end-users thanks to GeoIPS status as a tactical decision aide. Future research is suggested, and plans for possible continuance are discussed.

This page intentionally left blank.

REMOTE DETECTION OF OVERWINTERING FIRES

1. INTRODUCTION

1.1 Statement of Purpose and Background

In wilderness regions rich with peat, such as boreal forests, wildfires can present a multiyear threat (Rein and Huang 2020; Scholten et al. 2021). Fires thought to be extinguished, may have burned into the subsurface layer of peat and continue to smolder. If the smolder persists through the winter, the fire may reemerge when the surface snow has melted, and ice has mostly thawed. Such fires are known as overwinters and represent an emergent threat to Naval assets in boreal forests. Beyond the obvious destructive threat uncontrolled wildfires presents to Naval assets, overwinters can impact aerial visibility via aerosol and smoke injection. Additionally, melting of the permafrost above smolders presents a trafficability risk. Thus, being able to detect overwinters would lead to new strategic capabilities for the Navy and broader defense initiatives, and become a novel capability possessed by no other standing force.

It is, as of present, difficult to detect overwinters—many commonly used remote sensing sources struggle with the combination of snow, ice and seasonal cloud cover that obstruct views of the surface. Studies analyzing overwinters rely on conditional windows of opportunity, or post-facto information. For instance, it is possible to use infrared (IR) and visual (VIS) sensors to identify subsurface hot spots that may indicate a fire (Schroeder et al. 2014; Waigl et al. 2017). However, when clouds, thick smoke and snow are present this window of opportunity is blocked (Schroeder et al. 2008). In other cases, it is possible to identify dry spots on the land surface via use of a passive microwave radiometer (PMR; Wigneron et al., 2003), even through cloud cover. Unfortunately, this method fails when the soil itself is frozen due to frozen soil's distinct PMR signal (Schwank et al. 2004). Further, at present PMW are relatively coarse resolution. A possible mitigation to the resolution problem is synthetic aperture radar (SAR). SAR expands upon the capabilities of PMW by being higher-resolution capable of penetrating the ground and taking subsurface measurements at a significantly higher resolution (Kornelson et al. 2013). SAR instruments, however, are substantially more expensive to operate and what few platforms exist tend to have tight controls on data distribution and collection.

Regardless, it would be of immense utility for Naval assets if we were able to detect overwinters either as they began, as they burned into the subsurface, or prior to their emergence. With such knowledge we would be able to take intervening actions and extinguish the fires mitigating damage risks against Naval assets. To do so, I proposed a multifaceted, multispectral approach to detection utilizing a broadband of wavelengths across multiple instruments. Individually, each source discussed above is insufficient. It is possible, though, that a concerto of sources can overcome the weaknesses of its parts. For instance, IR and VIS can detect pre-thaw, post-snowmelt smoke and provide context for SAR investigations. IR and VIS may also be used in concert with SAR/PMW to detect thinned patches of snow and ice related to ongoing smolder. Thus, I believe there is merit in investigating a multispectral approach to detection of overwinters to attempt to identify an objective algorithm for remote detection. Such an algorithm would be a boon and could be implemented in a tactical decision aide (TDA) such as the Navy's Geolocated Information Processing System (GeoIPS) for tactical use.

Manuscript approved October 2, 2023.

1.2 GeoIPS

Analysis of the research conducted here was conducted primarily through the Navy's GeoIPS software (Camacho et al. 2022). GeoIPS, currently in operations at the Fleet Numerical Meteorology and Oceanography Center and non-Naval organizations like the National Oceanic and Atmospheric Administration, is rapidly becoming the Navy's go-to system for weather processing. Designated as the TeraScan replacement by 2025, GeoIPS is an open-source, extensible TDA designed to ingest, process and display satellite data from many sources. To achieve this goal, GeoIPS is composed of a series of common interfaces utilizing common Python packages. These include xarray for data arrays and metadata, and cartopy for map controls. GeoIPS places emphasis on portability and shareability through its plugin system. Through plugins, developers can port algorithms they create into GeoIPS without having to modify or interact with the main GeoIPS code. Presently, the base GeoIPS package includes readers and products for over 20 Satellite Data Records (SDR; Level 1) and Environmental Data Records (EDR; Level 2 and 3). GeoIPS is actively maintained and while several interfaces are considered matured, some will undergo changes over the next few years. This means some ongoing maintenance of newly developed plugins is required. At present, GeoIPS has no publicly available fire-related products though active development is underway on a fire-related cumulonimbus product at NRL Monterey. Likewise, GeoIPS also currently lacks non-tropical cyclone related PMW/SAR products. Thus, any techniques created in this study will represent novel capabilities for GeoIPS. These new capabilities can then easily be shared among other research and operational personnel.

2. APPROACH

2.1 Selected Remote Sensing Platforms and Data

For this project I chose to consider a broad spectrum of remote sensing platforms. Because I am targeting subsurface fires, I thought suitable instruments to be VIS (Smoke detection and burn scar evidence), IR (Detection of anomalous surface heat signatures), PMR (Direct interaction with the dielectric constants of surface soil) and SAR (Capable of direct, subsurface measurements.) While many such instruments are currently measuring the Earth from a variety of orbits, I required instruments capable of resolving spatially small events, on the order of tens of thousands of acres. Geostationary satellites (GEO), while able to take frequent observations, suffer from several constraints that preclude their use for this study. The first constraint is their resolution—given that they must maintain a higher-altitude orbit they are unable to provide suitable resolution for events that often consume only tens of thousands of acres. This has improved over time, with the latest Geostationary Operational Environmental Satellite (GOES) Advanced Baseline Imager (ABI; Schmidt et al. 2005) offering an unprecedented 0.5 to 1 km resolution in its visible channels. Its infrared channels however offer only 2 km resolution, or roughly 1000 acres, hamstringing the amount of information I can extract. Thus, modern, high-resolution low-earth orbiters (LEO) were selected. LEO, in contrast, fly at lower orbits and thus can achieve higher resolutions at the cost of 1 to 3 day return periods. That is, we can expect 2 passes per day of a LEO in each area, but then must wait several days before it returns. Given the slow nature of smolder progression, and the timeframes at which smolders operate, I believe this is of minimal concern.

The second constraint on GEO relates to view angles at high latitudes. Because GEO satellites must maintain a fixed orbit at the equator, their view of high latitudes becomes skewed, and some information can be lost, smeared out or even subject to parallax effects. In contrast, LEO consistently take observations either at- or slightly off-nadir (depending on the instrument) and suffer from skewing only on the limbs of the measurement. Given my needs, I identified two instruments suitable for this effort: the Visible Infrared Imaging Radiometer Suite (VIIRS; Murphy et al. 2006) on-board the Suomi National Polar-orbiting Partnership satellite (S-NPP) and the Soil Moisture Active Passive (SMAP; Entekhabi et al., 2010) SAR/PMR. I summarize both below.

2.1.1 VIIRS

The VIIRS instrument suite, which first launched aboard the S-NPP satellite in 2011, is a state-of-the-art, high-resolution (375m) thermal imager and moderate resolution (750m) infrared radiometer.

VIIRS was designated as the replacement of the Moderate Resolution Imaging Spectroradiometer (MODIS) and the Advanced, Very High-Resolution Radiometer (AVHRR) (Cao et al., 2013). VIIRS has 22 channels ranging from wavelengths of 0.41 micrometers to 12.01 micrometers. VIIRS has been used for fire assessment in the past owing primarily to four of its high-resolution imaging channels—Channels I1, I2, I4, and I5 (0.64 μm, 0.865 μm, 3.74 μm, and 11.45 μm respectively.) These channels can be combined with one another in ways that amplify fire and smoke signals from other features. For instance, Channel I4 is centered at the peak spectral radiance for blackbodies emitting at typical forest fire temperatures (Schroeder et al. 2014) and can be compared against I5 to discern burning pixels from background data. Channel I1, the imaging channel, is excellent for smoke and cloud detection. Channel I2, the Normalized Difference Vegetation Index (NDVI) channel is suited for further cloud detection, as well as burned or otherwise unhealthy vegetation discernment. It also can assist in discriminating a snow or ice backdrop which is of relevance for boreal winter. The imaging channels do have one weakness in that they require sunlight to be reflected from the target. Thus, they are generally only available in the day. There are some exceptions, however. Large fires burning at night should be detectable as they produce their own light. Further, work has been done to exploit lunar reflectance to add nighttime functionality. This is done with the VIIRS Day-Night Band.

While at a lower resolution, the moderate resolution infrared channels are also of great value for fire detection. Primarily, the IR channels are useful for discriminating clouds from smoke through a fusion of the 0.64 μm, 1.6 μm, 3.75 μm, 8,5 μm, 11.0 μm, and 12.0 μm channels. The reasons for this are like those listed above, just at a slightly coarser resolution and available at night. Because the IR instrument relies on the emissions of the body rather than reflected sunlight, heat signatures in the IR spectrum can be identified with these channels. This feature is useful for seeing things not readily apparent from visual inspection of a scene. Finally, combinations of the near infrared (NIR) and shortwave infrared (SWIR) channels (M11 and M7, respectively) can be used to measure the intensity of a burn against the background state. The moderate and high-resolution channels listed above are all used in this study; however, I would like to note that there is potentially value in exploring other channels beyond these for further refinement of my processes, detailed in Chapter 4.

2.1.2 SMAP

The SMAP instrument suite *included* both a PMR and L-band SAR and is primarily intended for soil moisture and ocean surface monitoring. I say included here because shortly after launch, in 2015, the SAR failed and was deemed unrecoverable. The PMR, however, continues functioning to this day. SMAP can measure soil moisture because of the L-band's ability to directly measure surface soil moisture (PMR) and volumetric/sub-surface soil moisture (SAR) through interactions with the soil's dielectric constant. SMAP's SAR was notable for offering moderate resolution (3 km) retrievals of volumetric soil moisture. SMAP's PMR on the other hand natively retrieves surface soil moisture at a coarse 36 km resolution. However, thanks to a post-SAR failure PMR disaggregation scheme developed by NASA, SMAP's PMR has been able to provide retrievals of surface soil moisture at a more useful 9 km resolution. I believe SAR/PMR to be of value for this project owing to its relationship with the soil dielectric constant. It stands to reason that an area of smolder will be hotter and subsequently dryer and less frozen than its surrounding environment during the boreal winter. The ability to discern a subsurface dry patch from a surrounding moist or frozen backdrop could potentially identify subsurface burns.

2.2 Development of New Technologies and Capabilities

The primary phase of the research required development of novel technologies and capabilities. Several pieces of new technology were required to facilitate analysis:

1. A tool for parsing the contents of KMZ-formatted Alaskan Wildfire Reports.
2. New Level 1 and 2 readers for GeoIPS

3. New Products and Colorbars for GeoIPS
4. Creation of a new data fusion system for GeoIPS.
5. A system for large, targeted acquisition of data used to analyze individual case studies.

The development of each is enumerated in detail in the sections below. I'd like to note here, as part of a broader philosophy toward tool development, that each was developed with portability in mind. All tools were developed in Python using open-source packages and can be posted on an internal code repository for those who may need it. Currently, I do plan to make the GeoIPS packages available as it currently has few capabilities related to fires and fire tracking. The only thing preventing that from happening immediately is a recent code revision that updated the GeoIPS plugins interface. I will discuss that further in Chapter 4.

2.2.1 ATFDPM - A Tool for Fire Detection and Perimeter Mapping

To isolate test cases from the broader Alaskan Wildland Fire Information Database (AWD) and identify candidate fires for analysis, a utility was required to parse and analyze the contents of the Zip-compressed KML files (KMZ). This utility, A Tool for Fire Detection and Perimeter Mapping (ATFDPM) was written in Python using the pyKML, shapely, Pandas and Matplotlib libraries. For this project I retrieved the KMZ containing the Fire perimeter information and historical fire center points found in FireHistoryOulines.kmz (FHO) and FireHistoryPoints.kmz (FHP), respectively, for the period 2016-2020. To begin, the KML files are extracted from the two KMZ using the *unzip* binary at the OS level. AWD KMZ files contain only the XSL formatting rules and KML file containing the perimeter and point information for their listed subjects. Both files are preprocessed in *pt1_fireHistKML.py* and *pt2_fireHistKML.py* to extract information into a unified, Pandas dataframe for easy parsing and value-extraction/data manipulation. A CSV file is then generated, and is ingested by *ATFDPM.py*, which contains the algorithm used to determine possible overwinters from the timing of fires as well as new fire perimeter proximity between years. The preprocessing and analysis techniques are discussed below.

The FHO contains most of the information used for construction of the fire database and is the target of the first preprocessing script *(pt1_fireHistKML.py*). The FHP, target of the second preprocessing step (pt2_fireHistKML.py) contains information on the timing and cause of fires. Relevant contents of each file and short descriptions are provided in Table 1:

Table 1 – Relevant Contents of the FireHistoryOutlines (FHO) and FireHistoryPoints (FHP) KMZ files available from the Alaskan Wildfires Database

Source	KML Class Name	Short Description	Use
FHO	AFSNUMBER DOFNUMBER USFSNUMBER	Unique identifier provided by one to three agencies (Alaskan Forest Service, Department of Forestry, and US Forest Service, respectively.)	Tracks unique fires in situations where proper names are identical across years, or within one burning season
FHO	NAME	Proper name given to fire, typically referencing location of occurrence	Provides context for fire and easy reference in human language
FHO	ACRES	Total estimated acreage burned by fire	Determines if fire can be resolved using chosen satellite data sets

FHO	PRESCRIBED	Flag to denote if fire was reported as a prescribed burn by either forest management or local interest	Removes fires that were intentionally started and may be near infrastructure
FHO	FPOUTDATE	Estimated date fire was extinguished	Determines when fire was extinguished
FHO	POLYGON	Linear boundary coordinates of fire perimeter	Visualizes fire perimeter, and compares perimeters across years
FHP	DISCOVERYD	Date fire was discovered and believed to have started	Determines start date of fire
FHP	GENERALCAU	General cause of fire	Filters out non-smolder fires
FHP	SPECIFICCA	Specific cause of fire (if known)	Filters out non-smolder fires

The preprocessing scripts directly ingest the KML files and use the pykml parser to create an iterable, dictionary-like object using XML 1.0 formatting. Using the class names from Table 1, information for each unique fire is iteratively extracted into the Pandas dataframe. Once information from all fires has been extracted, the table is sorted based on DISCOVERYD and exported using Panda's to_csv feature. DISCOVERYD is chosen as sorting criteria to ensure the record is presented linearly in time, which will be crucial for my next processing step. In cases where DISCOVERD is not defined, the entry is flagged, and the fire's start date is replaced with its FPOUTDATE. This is done under the assumption that for suitably small fires, the fire was extinguished shortly after discovery. Performance-wise, I observed both preprocessing steps to run relatively quickly, scaling in O(N) time with the record length of the inputs.

Next, the data are ingested into *ATFDPM*.py for filtering. In this script, the sorted list is read in, and the POLYGON entries are converted from a list of points to the shapely library's Polygon format. This will be used later when analyzing the results. The script then uses iteration to identify fires with overlap across sequential years using shapely's *intersect* function. As per the criteria identified in Scholten et al. (2021), the perimeter of the year prior's fire is extended by 1km in all directions to account for subsurface spread. As this process was found to be somewhat time consuming on large records, the results are then saved locally for fast recall in subsequent executions. After candidate fire pairs have been identified, I remove subsequent year fires that have known, non-overwinter causes (e.g., lightning or prescribed burns.) The reporting process for GENERALCAU and SPECIFICCA has no standard format or criteria, thus we had to manually identify categories for removal. These categories included human, debris burning, campfire, equipment, coal seam, firework, and firearm sources. It is possible that indirectly collected attributions are faulty, though it is unknown how to confirm or deny that assertion. Regardless, after this analysis I are then left with several candidate fires that can be analyzed, which I will discuss in Chapter 3 of this report. Additionally, *ATFDPM.py* also includes a small utility written for the cartopy and matplotlib libraries that creates quick looks of fire perimeters.

2.2.2 All New GeoIPS capabilities

In order to conduct the analysis using sources identified in Chapters 1 and 2 and ensure that any research performed as part of this grant could be shared, I created a new plugin for GeoIPS tentatively titled *overwinters*. This entailed the development of three readers, two new algorithms, and 10 new products. Two readers were somewhat novel applications of GeoIPS—one is (to my knowledge) the first use of GeoIPS to display SMAP radar sigma naught (S0) SDR data, and the other is a rare use of GeoIPS to display

an EDR product, the VIIRS cloud-mask product (CMASK). The third is a relatively simple reader for SMAP microwave radiometer brightness temperatures (MBT). The two algorithms I developed to compute normalized burn ratio (NBR) and VIIRS Day Cloud Fire RFB (SCARGB) are algebraic and RGB algorithms, respectively. Lastly the 10 products are display rules for the contents of the SMAP and VIIRS data, including a quaternary cloud map, with some overlapping use of colormaps. Each new GeoIPS capability is discussed briefly below.

a) *The SMAP Radar S0 Reader, Products and Colormaps*

SMAP Radar data were distributed in HDF5 files at 3km horizontal resolution. Relevant for GeoIPS are the aft- and fore-facing S0 values, which represent the backscatter coefficients obtained by the radar expressed in decibels (db). These values are available as two-dimensional cross-, vertical, and horizontal-polarizations. Latitude and longitude of the centroid of each scan and FOV are also available. Within GeoIPS, each variable is read into a simple numpy array and then passed to the main reader as a dictionary of xarrays, one containing metadata only, the other containing the variables. Scan times, required within GeoIPS, are served in a YYYY-mm-ddTHH:MM:SS string and can be decoded into a GeoIPS-compatible value through the datetime library. Lastly, the reader sets some standard metadata required for the product system, namely the source and platform names, start and end times, and data provider.

For colormaps, because I did not find any known display values for S0 data, a simple rainbow colormap developed by the National Corporation for Atmospheric Research Command Language (NCL) was used for each display. Such a colormap is high-contrast and useful for discerning features nested within other regions. Because GeoIPS allows for each product to supply arguments to the colormap function, only one colormap product was created. Valid minimum and maximum values were chosen for each product based on metadata contained within the HDF5 files. Products were created to display each of the following: s0_hpol_fore, s0_xpol_fire and s0_ypol_fore.

b) The SMAP MBT Reader, Products and Colormaps

SMAP on EASE grid resolution radiometer data (Kim et al. 2016) are distributed in HDF5 files at 9km horizontal resolution. As with the Radar S0 data, they are available from aft- and fore-facing angles and include relevant geolocation information. Different, however, are the available variables and configuration. Radiometer data are served as one-dimensional MBT and are available in horizontal and vertical polarizations. Additionally, the third and fourth Stokes parameter are available as MBTs. I note here that GeoIPS is equally capable of handling 1- and 2D variables, so no adjustments or regridding of the 1D MBTs into 2D is required. Somewhat similarly to the radar S0 data, scan times are in an easily parsed string format of YYYY-mm-ddTHH:MM:SS.fZ. All data are read in as numpy arrays and converted to the GeoIPS-formatted dictionary of xarrays. Additionally, the standard metadata are collected by the reader. For a colormap I used the same routine as the s0 colormap, implemented identically. Products were created to display the fore-facing H- and V-pol MBTs, as well as the 3rd and 4th Stokes Parameters.

c) The VIIRS Level 2 Cloud Mask Reader and Colormap

VIIRS Level 2 Cloud Mask data (Kopp et al 2014) files are distributed as NetCDF files on the 750-meter moderate resolution VIIRS grid. Unlike VIIRS IR data, geolocation is served natively within the product. I will expand on this comment in Chapter 2.2.4. This bypasses the need for the reader to account for split geophysical data and geolocation files. Of relevance to the reader is the quaternary Integer Cloud Mask, which is read in as a numpy array of integers and passed to the main reader as an xarray. Use of integer arrays here is particularly helpful for the high-resolution data as they substantially reduce the RAM used for execution. Scan times are served in 1D arrays in the International Atomic Time 1993 (TAI93) format. This presents serial problems for the CMASK reader, requiring both conversion to an acceptable datetime format and the addition of leap seconds to ensure accurate timing. Further, because the instrument

samples 16 scans simultaneously, the scan time variable's dimensions do not match the dimension of the Integer Cloud Mask. Thus, substantial preprocessing is required to convert the native VIIRS scan time record into one properly used by GeoIPS. To do so, I used the datetime library's timedelta option to add the modulo 16th index (MOD16) of the scan_start_time variable seconds to a starting time of 0000Z, 1-JAN-1993. MOD(16) ensures correct batching of the times so that the simultaneously captured scans have identical scan times. I also added 37 leap seconds to each scan, as per TAI standards. Once scan times have been preprocessed, they can then be formatted to the GeoIPS standard. Lastly, the reader scans the file attributes and collects the required metadata.

Colormapping for this product is quite simple, owing to its quaternary nature. Clear and probably clear values (3 and 2, respectively) are made transparent, while cloudy and probably cloudy (0 and 1, respectively) are made white and grey. In the future work section, I discuss applying an alpha channel to the probably clear and probably cloudy values to emphasize ambiguity created by the *probably* categories.

d) The Normalized Burn Ratio (NBR) Product and Colormap

The NBR Product is computed using the GeoIPS algorithm interface. The algorithm is provided the near infrared (NIR) and shortwave infrared (SWIR) channel data. From VIIRS these are channels 7 and 11, respectively. NBR is then calculated as:

$$\frac{(NIR - SWIR)}{(NIR + SWIR)} \qquad (1)$$

(Roy et al. 2006) This quantity is dimensionless and has a valid range of [-1, 1]. Any values outside of these bounds are masked (such values would be associated with unmasked fill values that unintentionally propagated through the data.) This algorithm uses the default GeoIPS Gaussian interpolator. Because this product can be quite sensitive to cloud cover, it is essential that it be paired with a CMASK. Thus, this product must be used with the new GeoIPS data_fusion system, which I will outline in 2.2.3.

The colormap is generated using GeoIPS's Python-based colormapper interface and is adapted from common uses of NBR across literature. Low values of NBR are associated with burns and thus are colored red, while high values are associated with strong vegetation presence and are colored green. Intermediary values are orange yellow. Within GeoIPS, the boundary values are specified at every 0.2, and gradients between values are generated using GeoIPS's built-in create_linear_segmented_colormap utility.

e) The Burn Scar Red-Green-Blue (RGB) Product (scargb)

The scargb product is adapted from the VIIRS Day Land Cloud Fire RGB recipe provided by the Cooperative Institute for Research in the Atmosphere (Seaman et al., 2023). An RGB is a type of algorithm where each component of an RGB triplet is computed using channel data scaled from 0-1. Optionally, a gamma correction can be applied to the data to enhance certain features of each channel. Numerically a gamma correction is expressed as:

$$GammaCorrection = Original^{\left(\frac{1}{\gamma}\right)} \qquad (2)$$

In this case, the red component of the algorithm is the Imager's Channel 4 data whose minimum is set to 273 K and whose maximum is capped at 333 K. Data outside this range are cropped to these values. A gamma correction of 0.4 is applied to these results. For the green component, Imager Channel 2 data is used, with no gamma correction. Lastly, the blue component uses Imager Channel 1 data with no gamma correction. Because RGB products are self-describing with respect to colormaps, no colormap needs to be created or specified in the product configuration. Further, no minimum or maximum display values need to be set.

2.2.3 The GeoIPS Data Fusion System

The latest version of GeoIPS adds a Data Fusion system, which allows the user to create overlays of data from independent sources. This requires some adjustments to the procflow system, detailed below, but still utilizes the standard GeoIPS interfaces. The user is required to invoke a data_fusion_procflow, and provide a final output format for their product. Currently only annotated imagery and clean imagery are tested, though it is likely that NetCDF output is possible. A singular sector file is specified, as in the single source procflow, containing a defined sector. A fusion product must be created, though this generally just contains the names of the base products being overlaid and controls for their colorbars. For the purposes of this study, I made a fusion product called nbr_layered, which combines the NBR and CMASK products and instructions to only display the colorbar for NBR. Following this, the user then specifies readers, files and product names for each layer of the image. The user can also specify the order in which the images are plotted, in a first-in-first-out ordering. One caveat is that each fusion source product must be use the clean_imagery format. This is a consequence of the current implementation of the data fusion system and may change with subsequent releases.

2.2.4 A System for Large Scale Data Acquisition Used to Analyze Case Studies

Once potential case studies have been identified by ATFDPM, data from sources outlined in Section 2 must be acquired. To do this dumbly (e.g., acquire all swaths from the period of fire incipience to conclusion of overwinter) would be disastrous, requiring hundreds of terabytes (TB) of data. Thus, I needed to be able to intelligently filter my downloads so that I only retrieved data that covers my regions of interest over the lifetime of the fire. Thankfully, both of SMAP and VIIRS are served by organizations aware of these concerns and offer robust download filtering (with caveats in the case of VIIRS products.)

SMAP S0 data are hosted by the Alaskan Satellite Facility through their Distributed Active Archive Center (DAAC). They offer a robust querying service through their Vertex Data Search Utility that allows the specification of polygonal regions. From the polygon and SMAP metadata, swaths intersecting the polygon are identified and a subset is produced. Data can then be further filtered by time and dataset collection to identify the exact subset of data required for a case study. This process is functionally identical for the SMAP MBT data on the National Snow and Ice Data Center DAAC, as well as the VIIRS SDR and CMASK data on NASA's DAAC. However, the VIIRS data do suffer from one particularly troublesome caveat that I needed to overcome.

Because VIIRS is incredibly granularized, and geolocation is separate from geophysical data, one fire's worth of data over a region can consist of thousands upon thousands of files. NASA's DAAC provides filtering like ASF and NSIDC, and stages requested data (which can be geographically and temporally subset in such a way that only the data required by the user are downloaded) as an order that is fulfilled by the DAAC. However, there is a hard limit of 2000 files that can be added to a single order. For context, one fire requires about 26,221 separate VIIRS files. Thus, some creative bypassing of the DAAC's limitations is required. To do so, I first identified where the full data sets were stored on the DAAC's server (this information is publicly facing, thankfully.) I then created an ordered that spanned the full life of the fire and contained all the data required for my analysis. The DAAC allows for this, and will only return a file limit error when attempting to stage the large order. Importantly, it produces a CSV containing the list of files to be downloaded, which that user can access. By writing a Python script that parses the CSV and correctly populates the server URL, one can directly fetch the requested data without the cumbersome 2000 file limit. Prior to discovering this technique, downloads would take weeks. However, afterwards fetching a fire's worth of data became a several-day task requiring no interaction.

Once the data were retrieved, I checked the VIIRS data for geolocation and geophysical parity, as the archive is imperfect and has a small amount of missing data. I did this because later down the processing chain I will automate generation of satellite products via bash scripting in a relatively simplistic, if not vulnerable method by iterating through the contents of the directory and assuming VIIRS files are ordered

correctly. This turned out to be significant, as some mismatching geophysical and geolocation files were found and removed from the directory.

2.3 Analytic approach

First, the archival version of the AWD fire history and outlines were retrieved from their public-facing HTTPS site. These were then run through the ATFDPM to extract overlapping fires. Fires whose total burned acreage could be resolved by the VIIRS IR instrument's 750m resolution (that is, fires with burned acreage > 139 acres) were selected. Once candidates were identified, SMAP and VIIRS data for the incipient and possible overwintering fire were retrieved. Unfortunately, no fires uniquely identified by ATFDPM overlapped with the lifetime of the SMAP radar instrument, severely limiting the number of cases able to be studied with SAR. I believe this to have a deleterious effect on overall analytical capabilities. To compensate, a fire from Scholten et al. (2021) that meets the acreage requirements was selected. This fire occurred in the Canadian boreal forests in 2014 and was outside the record used by ATFDPM. However, because the dynamics of overwintering are similar for all boreal forests, this should not significantly impact any conclusions that are drawn.

From ATFDPM, three candidate fires were identified. The only fire that met the spatial criteria started on May 30th, 2018, as a prescribed burn, titled DTAW Oklahoma Impact Area RX 2018 (DOIAR2). The FPoutdate was not specified in the original record and was assigned an identical start/end date, lending some ambiguity to the nature of the overwinter I hope to resolve. Regardless over its lifetime the incipient fire covered 25,851 acres. Its perimeter (extended by 1km for overlap detection) can be seen shaded in red in Fig. 1 below. The subsequent year, beginning on April 30th, a fire abutting the perimeter (see the area shaded blue in Fig. 1 below) of DOIAR2 emerged, and burned a total of 34,741 acres, finally being extinguished on October 3rd, 2019. This fire was given the name Oregon Lakes, and was not listed as a prescribed burn, and causes were indeterminate.

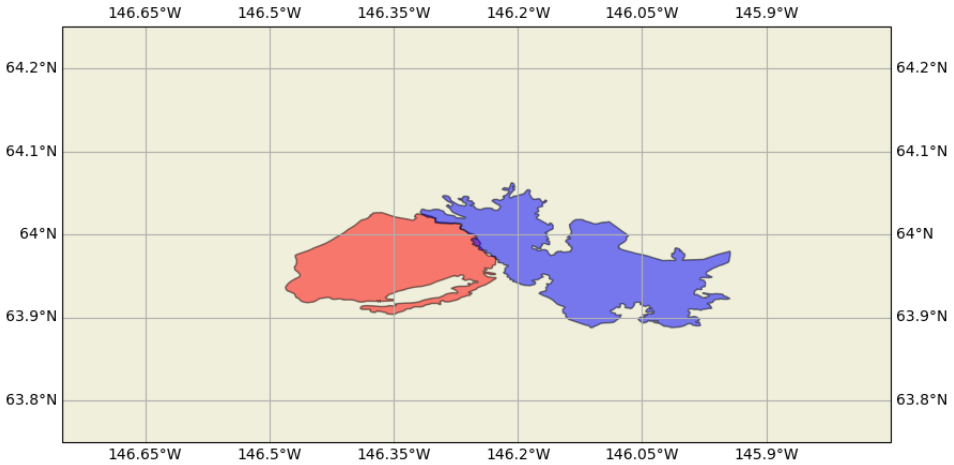

Fig. 1 – Shaded area of incipient fire (DTAW Oklahoma Impact Area RX 2018, red) and potential overwintering fire (Oregon Lakes 2019, blue). Overlapping areas are shaded in purple.

Once Identified by ATFDPM, and for the fire identified in Scholten et al. (2021) I retrieved data leveraging the technique outlined in 2.2.4 for the total lifetime of both fires. That is, I retrieved data from the incipient fire's beginning to the extinguishing of the possible overwinter. In total, the datasets for both fires totaled 5.2 TB, and required a period of several weeks to retrieve. Data were sorted by source, and bash scripts were created to generate the full suite of GeoIPS products created for this project, which took an additional several weeks of processing time. In total, 5208 images were produced. Note this value seems lower than the total number of files retrieved would suggest. This is because GeoIPS does not produce imagery when

regional coverage is below a certain threshold. When the products were generated, I began looking over them, attempting to visually identify potential features that could later be exploited for algorithmic detection of overwinters, and identify candidate channel combinations for better spatial analysis. My findings are summarized in section 3.

3. EXPERIMENTS

3.1 Scholten et al. (2021) Fire

The fire from Scholten et al. (2021) began August 3rd, 2014, around 2012Z (Fig. 2, highlighted box) nested among many other fires. Active fires in the scargb product are represented as bright red pixels. Burn scars are brown and dark red pixels. Smoke can also be identified as a thin, blue wisps or plumes.

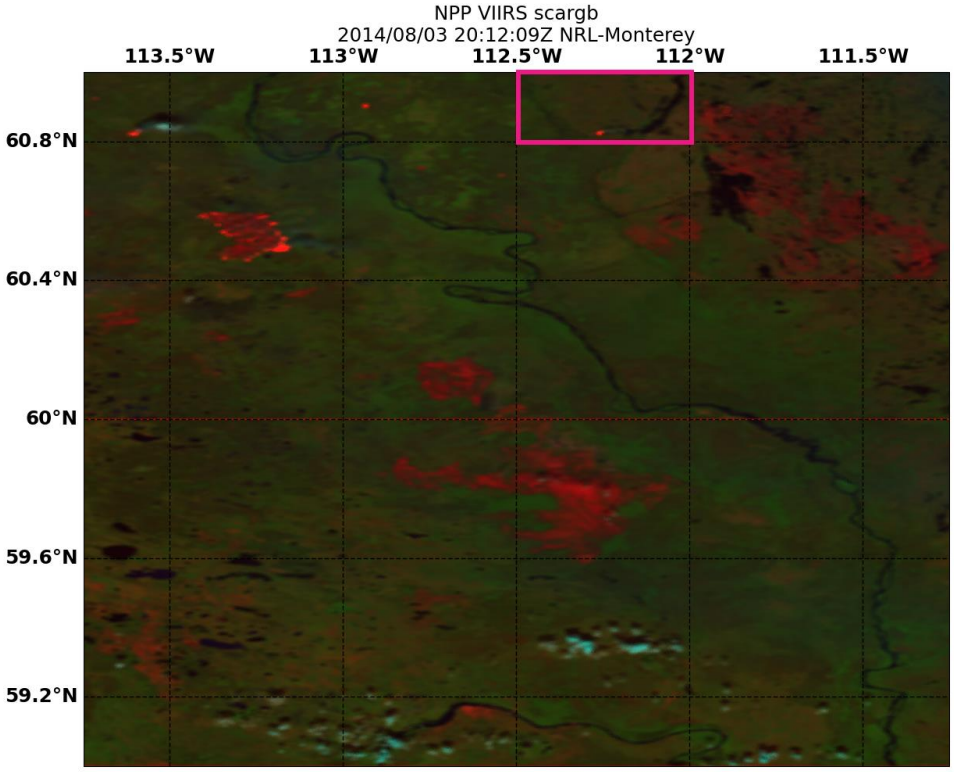

Fig. 2 – Incipient stage of the overwinter identified in Scholten et al. (2021)

The fire progressed steadily over the next several days (Fig. 3):

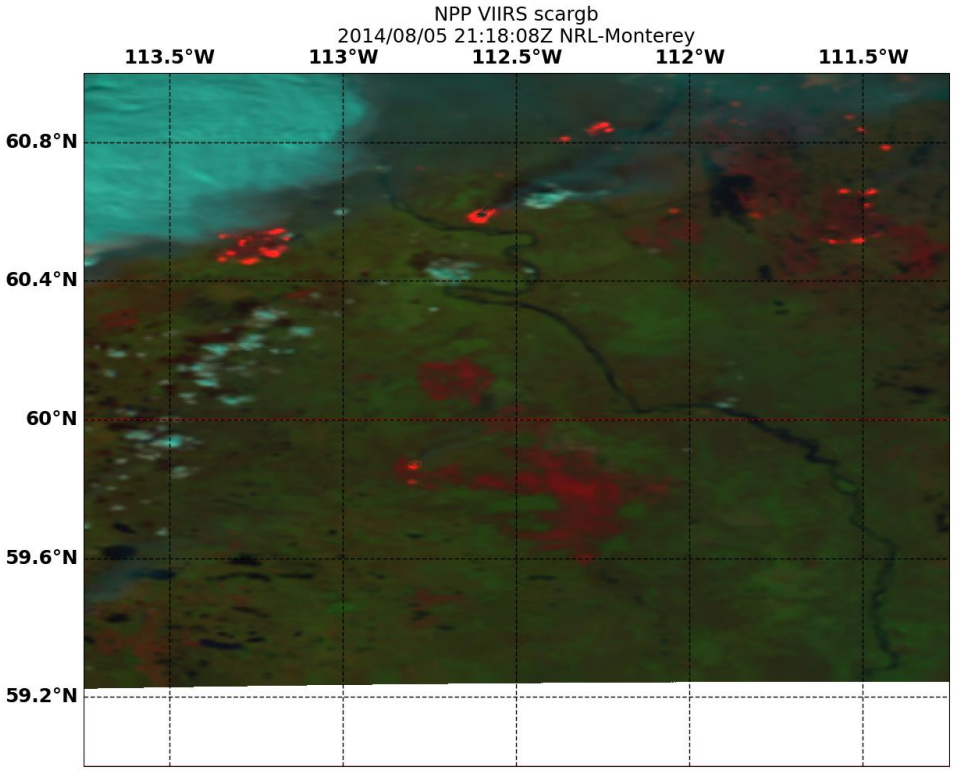

Fig. 3 – Progressive stage of the fire

Before being extinguished after a short re-flaring by the 20th of August. Whilst unrelated to the overwinter of Scholten et al. (2021), I want to call attention to the other large, nearby fires to the South and West. These will become relevant in future images. Returning to the overwinter of Scholten et al. (2021), unbeknownst to the fire teams on the ground the fire continued to smolder in the subsurface peat, and continued to do so until the fire resumed on May 30th of 2059 (Fig. 4) and burned intensely (Fig. 5) until again being extinguished around the 31st of May:

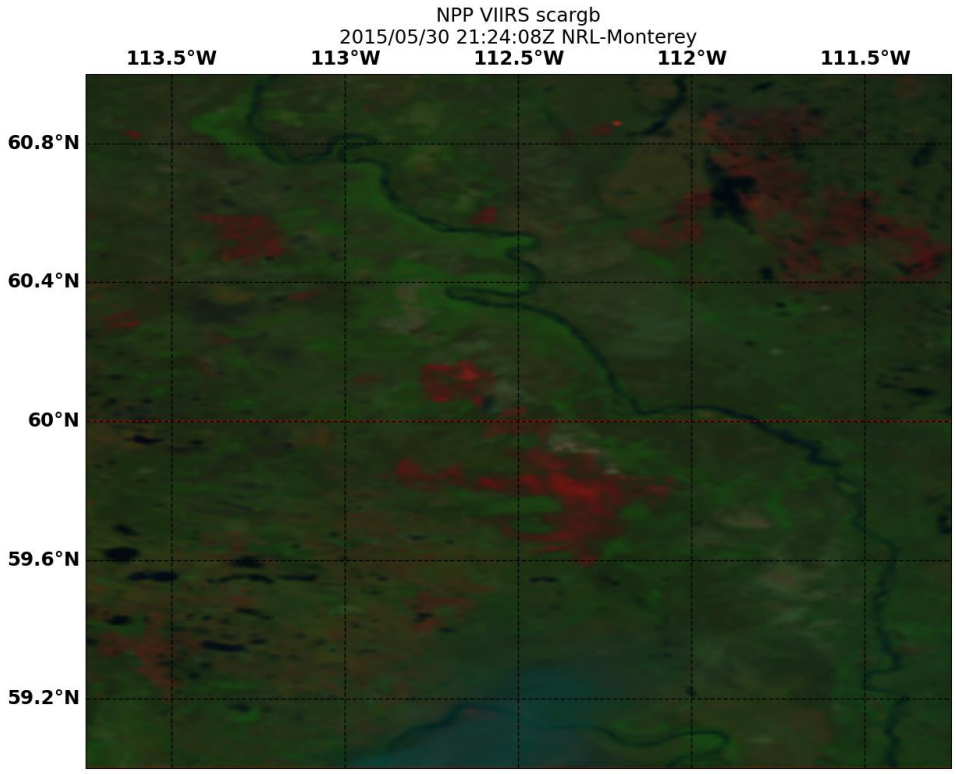

Fig. 4 – Overwinter resumes

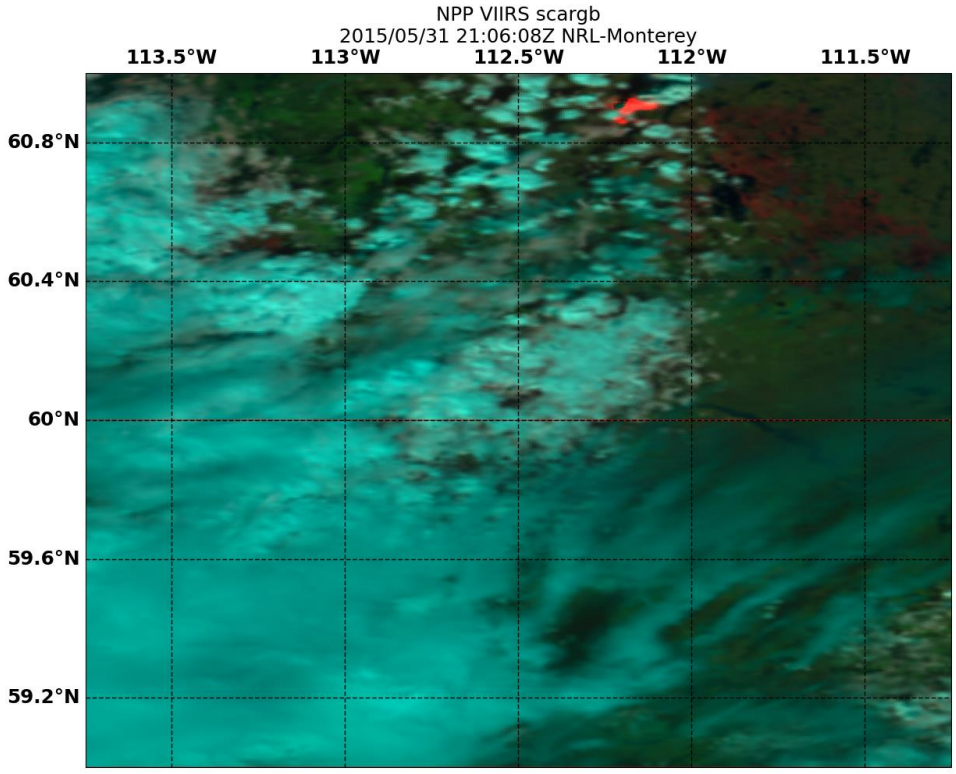

Fig. 5 – Overwinter burns hard

After constructing this timeline, I perused each generated product image in a gallery style to visually identify if any features in the products appeared in the proximity of the source fire and then persisted across

the winter months. As mentioned in Chapter 2, for SMAP I was somewhat limited by the operational lifetime of the SAR instrument, as data only became available in early April. Thus, I was only able to analyze the no-snow, pre-thaw conditions for this fire using both PMW and SAR. From SAR, no consistent features were discernable specifically related to the overwinter itself. While there is a somewhat persistent high value in the region of the fire, it stands to reason that it is more related to the presence of a burn scar. I have some proof for this claim because high values persist over burn scars from the previously mentioned unrelated fires that are not identified as overwintering also appear in many images (Figs. 6, 7):

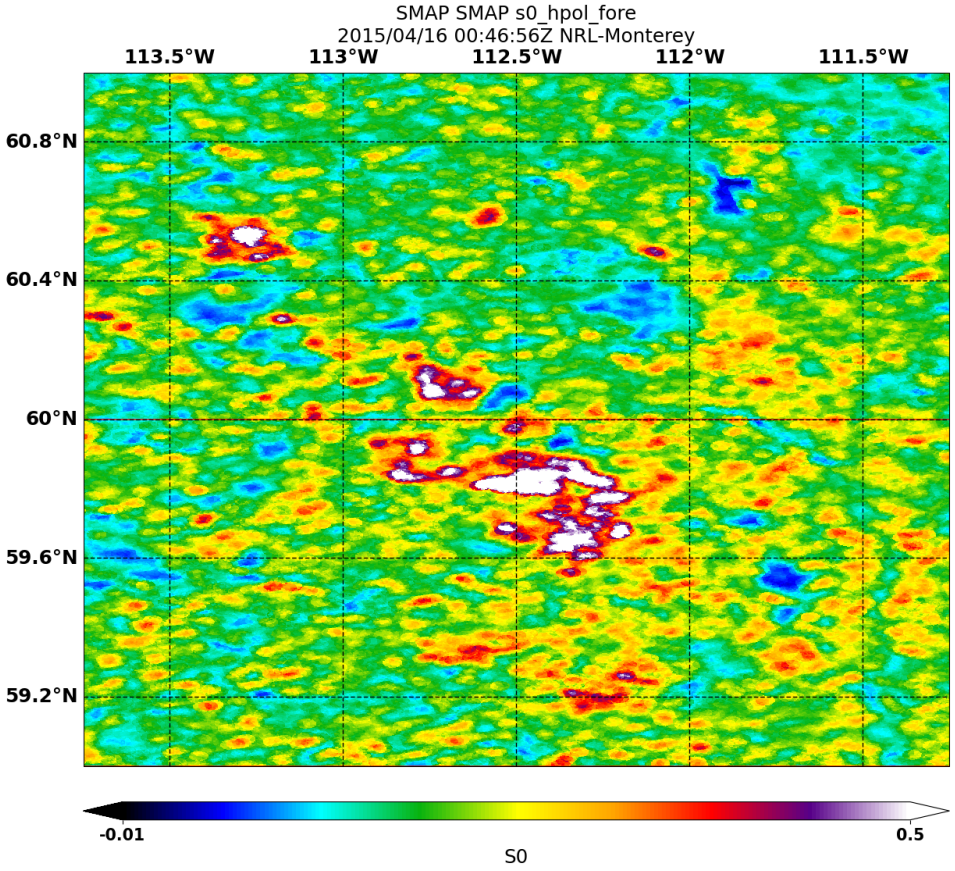

Fig. 6 – Burn scars from the prior year appear pronouncedly in this image. The overwinter also has a small region of high values that consistently appear.

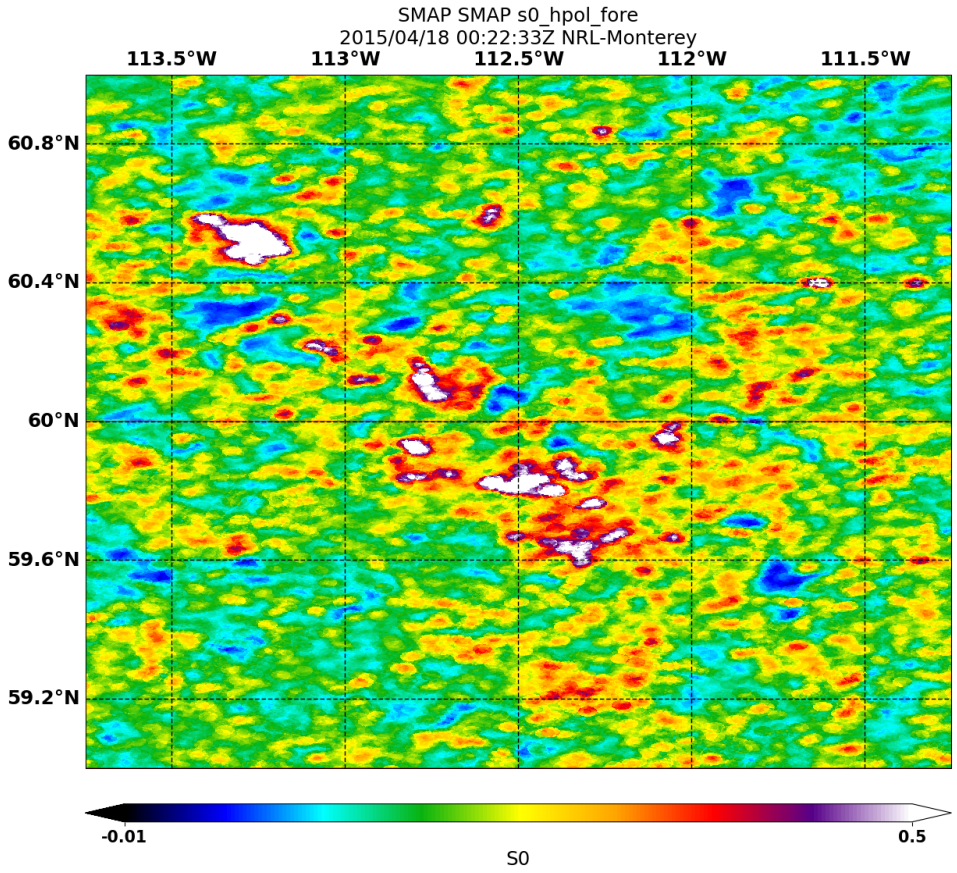

Fig. 7 – Burn scars appear in multiple images

Even more intriguing is the lack of high positive values associated with the burn scar of the fire in the Northeastern portion of the image. This prompts the question (not explored within this study) of why some scars are detectable by SAR while others are not. Given the penetrative qualities of SAR, it is possible this is associated with burn depth, though again this is based purely in speculation.

Regardless, failing to identify uniquely notable features of overwinters within SAR, I turned to the PMW. Upon perusing I discovered two issues: 1) the resolution of PMW is unsuitable for analysis of these small overwinters, and 2) no consistent features beyond those noted above were identifiable with any fire. I chose to look at the third and fourth Stokes parameters of the PMW measurements to see if the additional polarizations would display features. Unfortunately, the patterns of the third and fourth Stokes parameters revealed no consistent patterns and appeared to be mostly noisy (Fig. 8):

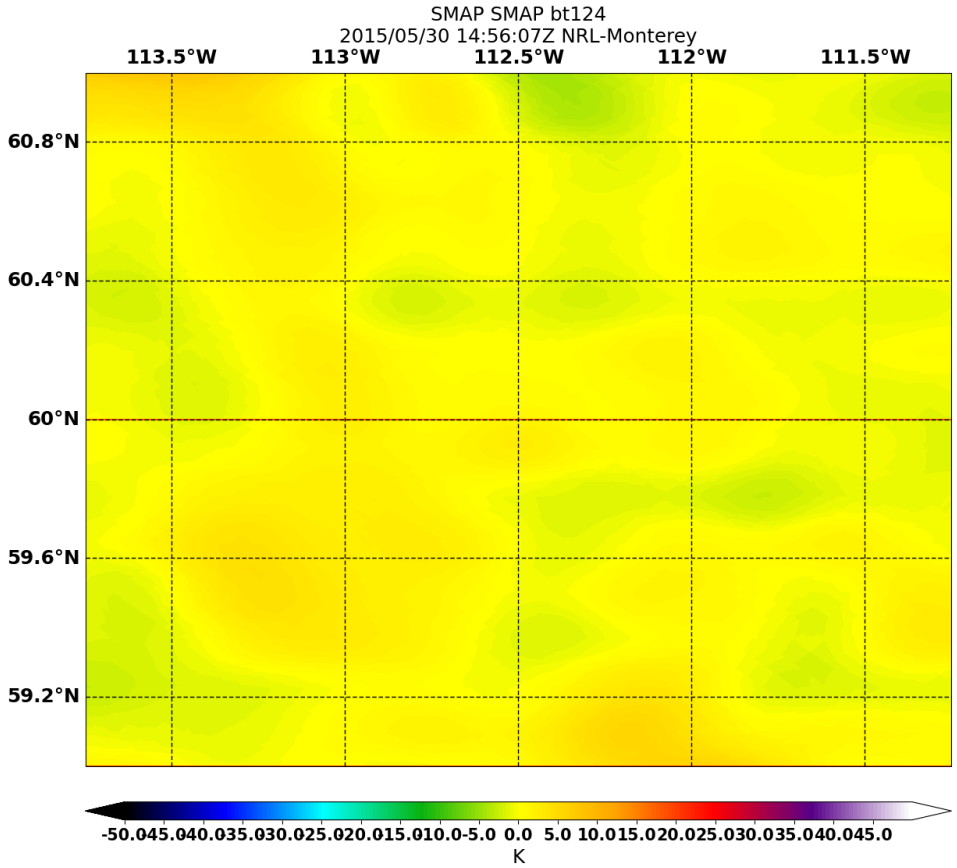

Fig. 8 – Fourth Stokes Parameter of the scene. No obvious features appeared across the collection of images.

Lastly, I'd like to note that the NBR product works as a corroboration technique for identifying burn scars as well as presently active fires. In Fig. 9, I can see the burn scars of several fires, including the fire in the Northeast not identified by the SAR product:

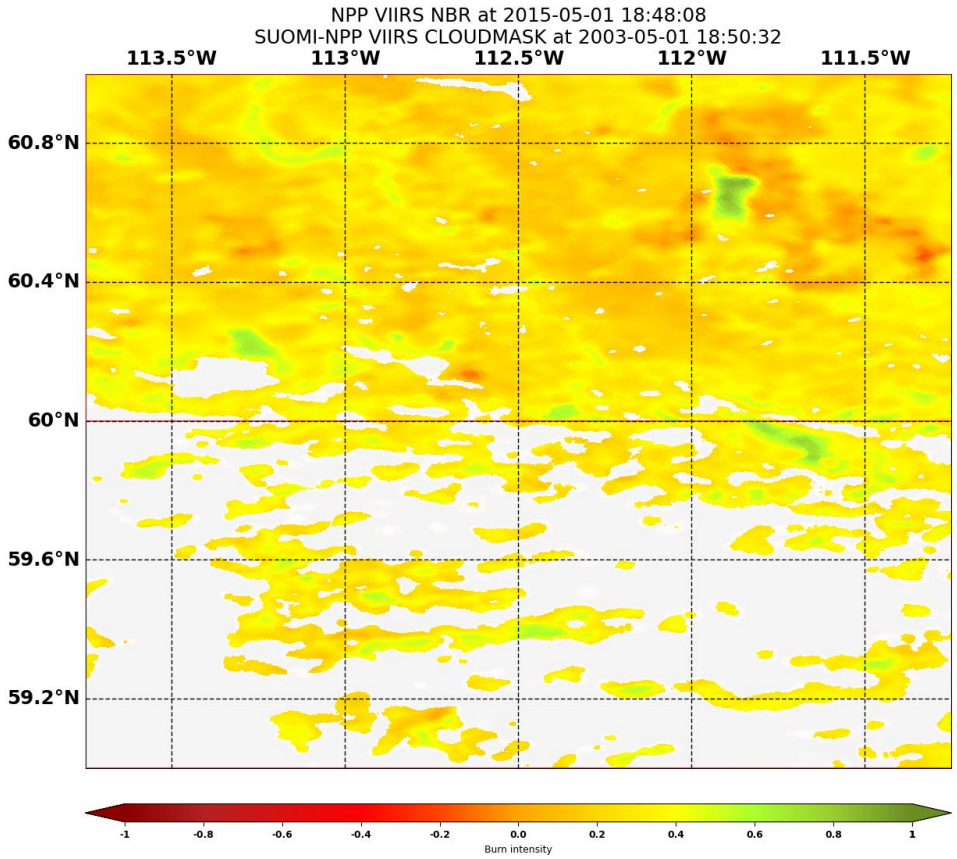

Fig. 9 – NBR product identifies burn scar of large fire in the NE, small fire in the N and mid-sized fire in the W. Masked values are under cloud cover.

The NBR product however does not provide any information about overwintering fires and thus, for the purposes of this work is used only as an identifying tool. From the images provided, it does appear that I have not yet been able to identify any characteristics of overwintering fires that can be used in remote detection. This is not a total loss, as I will expand upon in the next section as well as Chapter 4, however.

3.2 ATFDPM Fire

In contrast to the fire identified in Scholten et al. (2021), I do not have visual confirmation of the fire's incipient or progressive stages on May 30th of 2018. This is largely owed to cloud cover obstructing view of the fire, as well as pronounced limb effects from indirect passage. However, I can identify the fire's burn scar, shaded dark red, as evidenced in Fig. 10 below, highlighted in purple.

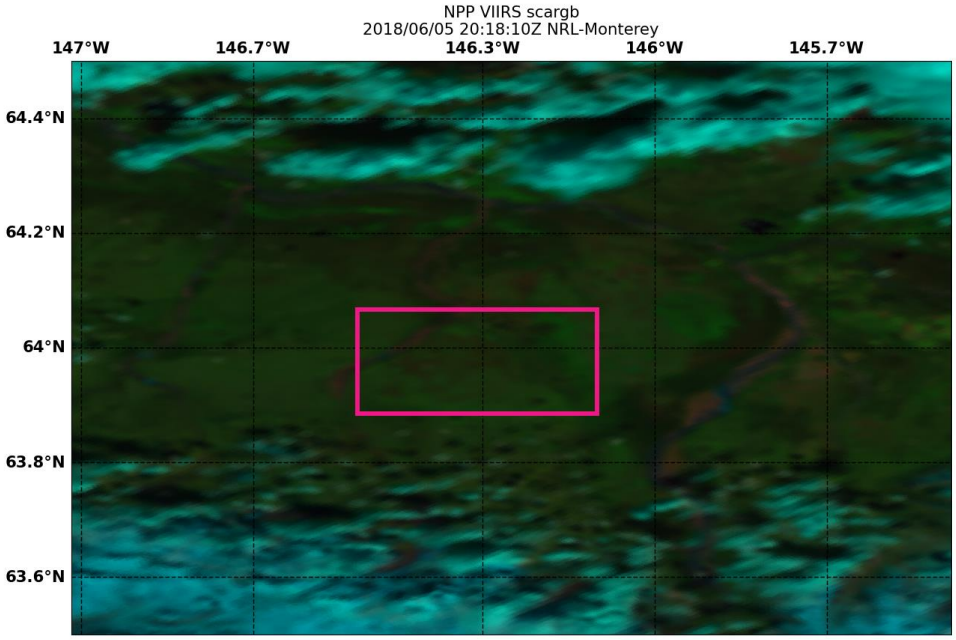

Fig. 10 – Burn scar of the ATFDPM fire identified by the scargb product

The following year, on April 30th, I saw a new fire had sparked a short distance away from the perimeter of the original (Fig. 11):

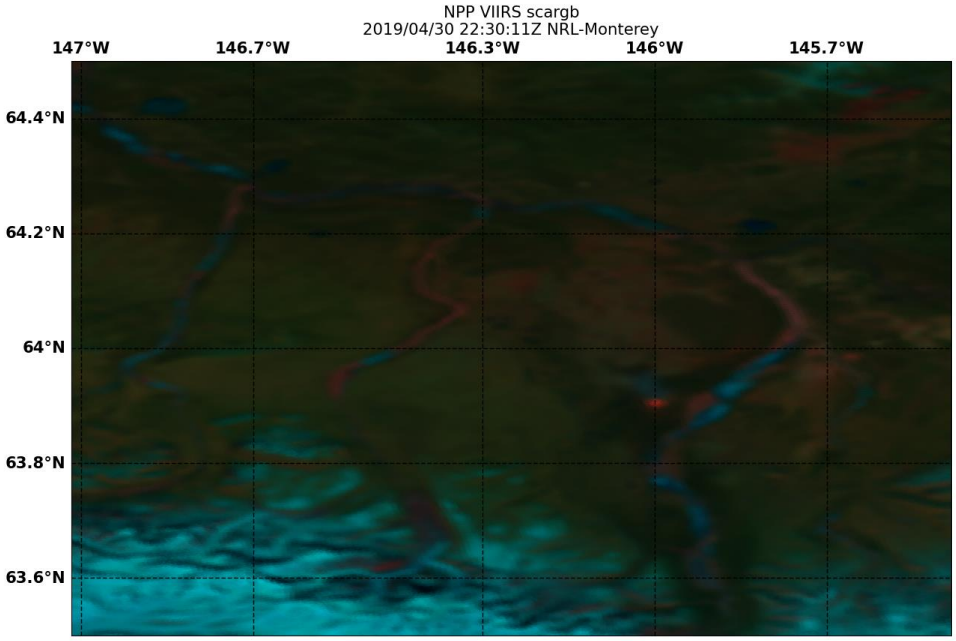

Fig. 11 – Potential resumption of an overwintering fire

While I established in 3.1 that my techniques are likely not suitable for detection of overwinters, I still chose to peruse the images to determine if any useful features could be discerned from the NBR or PMW data. Reminder that this fire occurred outside the lifespan of the SMAP SAR, and while suitable replacement instruments exist (e.g., the Japanese PALSAR-2), none have publicly accessible data in this region. I would thus have to rely on SMAP's PMW instrument, which given its 9km resolution, was ultimately unsuited to resolve the small and slow-moving subsurface fires related to an overwinter (Fig. 12):

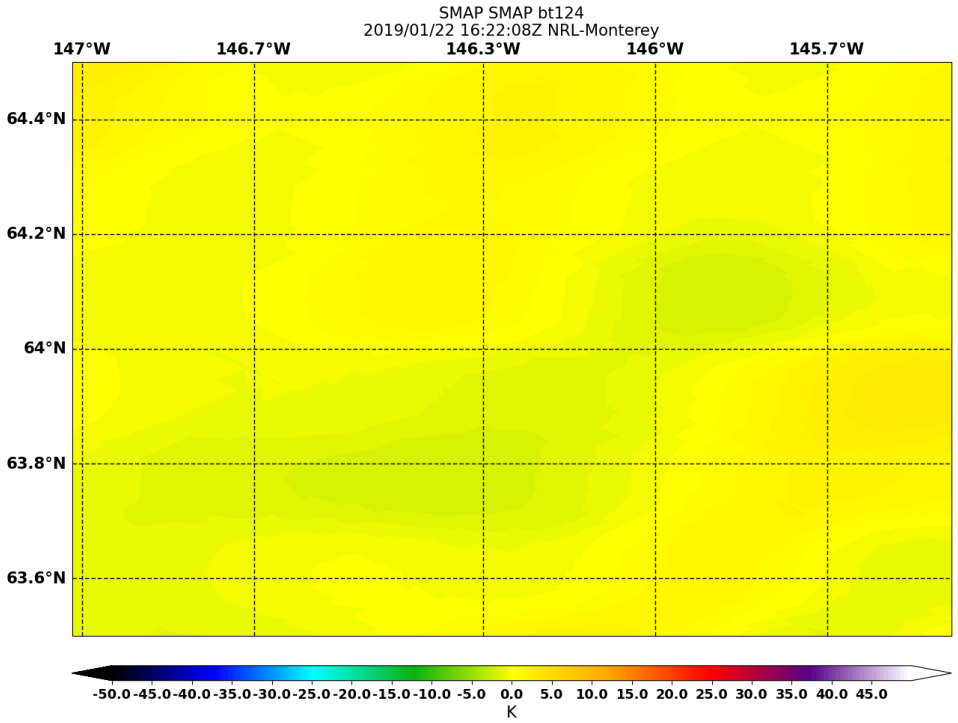

Fig. 12 – Sample image produced by SMAP PMW taken midwinter. Note the instruments resolution is too coarse to resolve small-scale features and is unsuited for overwinters.

I was, however, able to successfully detect the possible resumption of the fire the following year using the NBR and cloud-mask product, shown in Fig. 13 below:

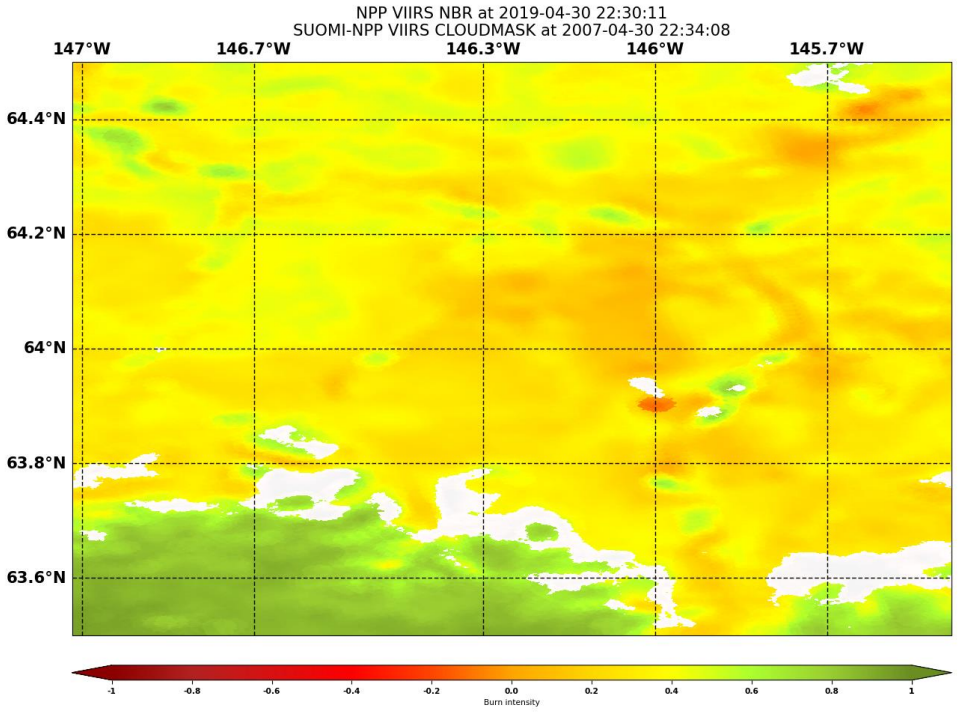

Fig. 13 – Clear NBR imagery of the potential resumption of a fire

Thus, while the techniques developed in this study are not yet suited for detecting overwintering fires, they are able to detect new and emerging fires. While this is not a novel capability in the field of remote

fire monitoring, it is a novel capability for GeoIPS, which as mentioned is poised to become a significant TDA for Naval activities. I discuss the implications of this more in the following Chapter.

4. CONCLUSIONS & SUGGESTED FUTURE WORK

Based upon the above results additional development and analytic effort will be required for detection of overwintering fires. While a great deal of new capabilities are now available within GeoIPS, objective detection of overwinters remains out of reach. This is mostly due to insufficient and inconsistent remote observation capabilities, needing further algorithmic analysis and new capabilities, and the topic was perhaps too demanding for a yearlong project. For the first concern, it's my hope that soon additional SAR instruments will become available. More so than just the L-band SAR that SMAP represents, I also hope for X- and C-band SAR as they may provide additional information to assist with detection. I further hope that in the future higher resolution PMW instruments will also become available as they are of particular use for surface detection of the dielectric constant of soil. Additionally, future work on this topic should broaden the instrument selection to also include hyperspectral data. Given the number of useful infrared channels for monitoring surface characteristics, it is possible that focusing on a range of wavelengths between those values could reveal additional features suitable for overwinter identification.

For the second concern, once a reasonable number of high-resolution sensors are available, we will need to perform further analysis on a broader spectrum of products. In the meantime, identification of more candidate overwinters over periods that coincide with the best instrument coverage is recommended. This can be done by enhancing ATFDPM to process a larger record of fires than the one used for this study, incorporating more information on the 3D characteristics of fire, and adding meteorological considerations including lightning and freeze/thaw. A similar approach is recommended to the one established in this paper, involving subjective analysis of many images to identify targetable features and then targeting them for algorithmic analysis. This entails creating new RGBs and algorithmic products that exploit the characteristics of wavelengths outside those mentioned in Chapter 2. It is likely that they could provide some mitigating factors that help to isolate the subsurface characteristics of overwinters from other fires.

However, all is not without hope for the existing work. Incipient and resuming fires can be cleanly detected via the scargb product as well as the NBR algorithm in GeoIPS. This is an important capability for Naval resources in regions across the globe. Given GeoIPS position as a TDA this capability could be natively integrated into the operational flow. Further, with these features identifiable visually, work can be done to objectivize the algorithms and create automated utilities that ping a central location to inform operators to the presence of a wilderness fire. To do so will require some filtering of the data and identification of local maxima/minima within both the scargb and NBR products. Further, the ability of SAR to detect pre-existing burn scars merits further investigation. This is not a commonly identified feature in literature, and there could be additional value added to post-fire characterization. This is especially in the context of some scars appearing in SAR data and others not. One might wonder if this has to do with burn depth given SAR's ability to penetrate the subsurface layers, though again this is speculation. Regardless, I do believe there is merit in continuing and broadening the scope of this work and hope to do so in the future when instrumentation is better suited to the task.

Some future work related to the GeoIPS interfaces is also suggested. Midway through this project's lifecycle there were substantial updates to the GeoIPS interfaces that will need to be applied. The major one is a restructuring of the directory structure. Instead of the hierarchy being PLUGIN/interface_modules/SUBJECT, the structure is now PLUGIN/plugins/modules/ for Python-based modules and PLUGIN/plugins/yaml for YAML-based plugins. In the context of this work, the new readers and algorithms will have to be adapted for the module-based approach, and the quaternary cloud mask and miscellaneous PMW/SAR products will have to be converted to the YAML-based approach. This has some benefit in cleaning up the readability of the code as each PMW/SAR product can share default configurations. Once these changes are implemented the plugin can then be open-sourced. Further work is also suggested in adding the ability to GeoIPS to read in multiple files and allow data manipulations from external sources within a product. In this context, this would allow creation of a delta-NBR (DNBR which is even better suited for discovering burn scars and new fires. Presently, I cannot read in a base NBR and

then subtract the instantaneous NBR from it to produce DNBR using just the GeoIPS interfaces. It would be possible to do this by reading a file within a DNBR algorithm, though this approach is somewhat clumsy and defeats the GeoIPS philosophy. Adding this capability is currently in the GeoIPS milestones.

REFERENCES

1. Cao, C., J. Xiong, S. Blonski, Q. Liu, S. Uprety, X. Shao, Y. Bai, F. Weng, 2013, "Suomi NPP VIIRS sensor data record verification, validation, and long-term performance monitoring," Journal of Geophysical Research: Atmospheres 118.20, 11-664.

2. Camacho, C. P., M. L. Surratt, S. Yang, 2022, "The Geolocated Information Processing System (GeoIPS)–A Platform for Collaborative Development," AGU Fall Meeting Abstracts. Vol. 2022.

3. Entekhabi, D., et al., 2010, "The soil moisture active passive (SMAP) mission," Proceedings of the IEEE 98.5, 704-716.

4. Kim, S., J. Van Zyl, R. S. Dunbar, E. G. Nijoku, J. T. Johnson, M. Moghaddam, L. Tsang, 2016 "SMAP L2 Radar Half-Orbit 3 km EASE-Grid Soil Moisture, Version 3." Boulder, Colorado USA. NASA National Snow and Ice Data Center Distributed Active Archive Center. doi: https://doi. org/10.5067/J8SGO1E0Y9XZ.

5. Kopp, T. J., W. Thomas, a. K. Heidinger, D. Botambekov, R. A. Frey, K. D. Hutchinson, B. D Iisager, K. Brueske, B. Reed, 2014, "The VIIRS Cloud Mask: Progress in the first year of S-NPP toward a common cloud detection scheme," Journal of Geophysical Research: Atmospheres 119.5, 2441-2456.

6. Kornelsen, K. C., P. Coulibaly, 2013, "Advances in soil moisture retrieval from synthetic aperture radar and hydrological applications," Journal of Hydrology 476, 460-489.

7. Murphy, R. E., P. Ardanuy, F. J. Deluccia, J. E. Clement, C. F. Schueler, 2006, "The visible infrared imaging radiometer suite," Earth Science Satellite Remote Sensing: Vol. 1: Science and Instruments. Berlin, Heidelberg: Springer Berlin Heidelberg, 199-223.

8. Rein, G., X. Huang, 2020, “Smouldering Wildfires in Peatlands, Forests and the Arctic. Challenges and Perspectives,” Current Opinion in Environmental Science & Health 24, doi:10.1016/j.coesh.2021.100296.

9. Roy, D. P., L. Boschetti, S. N. Trigg, 2006, "Remote sensing of fire severity: assessing the performance of the normalized burn ratio," IEEE Geoscience and remote sensing letters 3.1, 112-116.

10. Schmit, T. J., M. M. Gunshor, W. P. Menzel, J. J. Gurka, J. Li, A. S. Bachmeier, 2005, "Introducing the next-generation Advanced Baseline Imager on GOES-R," Bulletin of the American Meteorological Society 86.8, 1079-1096.

11. Scholten, R. C., R. Jandt, E. A. Miller, B. M. Rogers, S. Veraverbeke, 2021, “Overwintering Fires in Boreal Forests,” Nature 593, 399-404.

12. Schroeder, W., I. Csiszar, J. Morisette, 2008, "Quantifying the impact of cloud obscuration on remote sensing of active fires in the Brazilian Amazon," Remote Sensing of Environment 112.2, 456-470.

13. Schroeder, W., P. Olivia, L. Giglio, I. A. Csiszatr, 2014, "The New VIIRS 375 m active fire detection data product: Algorithm description and initial assessment," Remote Sensing of Environment 143, 85-96.

14. Schwank, M., M. Stahli, H. Wydler, J. Leuenberger, C. Matzler, H. Fluhrer, 2004, "Microwave L-band emission of freezing soil," IEEE Transactions on Geoscience and Remote Sensing 42.6, 1252-1261.

15. Seaman, C. J., W. Line, R. Ziel, J. Jenkins, C. Dierking, G. Hanson, 2023 "Multispectral Satellite Imagery Products for Fire Weather Applications." Journal of Atmospheric and Oceanic Technology.

16. Waigl, C. F., M. Steufer, A. Prakash, C. Ichoku, 2017, "Detecting high and low-intensity fires in Alaska using VIIRS I-band data: An improved operational approach for high latitudes." Remote Sensing of Environment 199, 389-400.

17. Wigneron, J-P., J. C. Calvet, T. Pellarin, A. A. Van de Griend, M. Berger, P. Ferrazzoli, 2003, "Retrieving near-surface soil moisture from microwave radiometric observations: current status and future plans," Remote Sensing of Environment 85.4, 489-506.